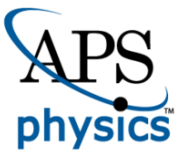

Quantum phases of Bose-Bose mixtures on a triangular lattice

Liang He, Yongqiang Li, Ehud Altman, and Walter Hofstetter

Phys. Rev. A **86**, 043620 — Published 19 October 2012

DOI: 10.1103/PhysRevA.86.043620

Quantum phases of Bose-Bose mixtures on a triangular lattice

Liang He[1], Yongqiang Li[1,3], Ehud Altman[2] and Walter Hofstetter[1]
[1] *Institut für Theoretische Physik, Goethe–Universität, 60438 Frankfurt/Main, Germany*
[2] *Department of Condensed Matter Physics, The Weizmann Institute of Science, Rehovot 76100, Israel and*
[3] *Department of Physics, National University of Defense Technology, Changsha 410073, P. R. China*

We investigate the zero temperature quantum phases of a Bose-Bose mixture on a triangular lattice using Bosonic Dynamical Mean Field Theory (BDMFT). We consider the case of total filling one where geometric frustration arises for asymmetric hopping. We map out a rich ground state phase diagram including xy-ferromagnetic, spin-density wave, superfluid, and supersolid phases. In particular, we identify a stripe spin-density wave phase for highly asymmetric hopping. On top of the spin-density wave, we find that the system generically shows weak charge (particle) density wave order.

PACS numbers: 67.85.Hj, 67.60.Bc, 75.10.Jm, 67.85.Fg

I. INTRODUCTION

Geometric frustration arises when magnetic interactions between different spins on a lattice are incompatible with the underlying crystal geometry. Since the first investigation of the Ising antiferromagnet on the triangular lattice [1], geometric frustration has been a constant source of surprises that inspired the development of new concepts [2, 3]. This provides strong motivation to study the physics of frustration from the different perspective provided by systems of ultra-cold atoms.

Recent experiments have made substantial strides in this direction with the realization of non-bipartite triangular [4, 5] and kagome [6] optical lattices. In this paper we investigate the consequence of bringing a two component bosonic mixture into the Mott insulating regime on the triangular lattice. Deep in the Mott state, the magnetic exchange interactions can include as the main source of frustration a strong Ising antiferromagnetic exchange.

Our goal is to study how the magnetic phases evolve when we increase the frustrating Ising interaction or approach closer to the transition to the superfluid phase, such that the effective spin model with second-order exchange interactions no longer applies.

To answer this question we apply Bosonic Dynamical Mean Field Theory (BDMFT) [7–9], which is non-perturbative in the hopping amplitudes. We find that even in the deep Mott regime, the standard spin exchange model is invalid for extremely asymmetric hopping. Instead, we numerically identify a stripe spin-density wave (SDW) phase (see Fig. 1a.2). This can be understood within a higher-order effective spin-model (8) derived from fourth order perturbation theory. The effective description shows that the stripe SDW is favored by the higher-order density fluctuations of the "lighter" atoms which remove the Ising-type frustration. Moreover, we also find that on top of the spin-density wave, due to asymmetry of the hopping amplitudes, the system develops a weak charge-density wave in the total particle density (see Fig. 3).

The paper is organized as follows. In Sec. II, we introduce the system and model studied here, as well as the theoretical approach used in our investigation. In Sec. III, the main part of this paper, we present a detailed discussion of the ground state properties of the system. We conclude in Sec. IV.

II. MODEL AND METHOD

We consider two species (hyperfine states or isotopes) of ultracold bosons loaded into a triangular optical lattice. For sufficiently low filling this system can be described by a two-component Bose-Hubbard model in the lowest band approximation:

$$\begin{aligned} H &= -\sum_{\langle i,j\rangle}(t_a a_i^\dagger a_j + t_b b_i^\dagger b_j + \text{h.c.}) + U\sum_i n_{ai} n_{bi} \\ &\quad + \frac{1}{2}\sum_{i;\alpha=a,b} V_\alpha n_{i\alpha}(n_{i\alpha}-1) - \sum_{i;\alpha=a,b}\mu_\alpha n_{\alpha i}\,. \quad (1) \end{aligned}$$

Here $\langle i,j\rangle$ denotes nearest-neighbor sites, $a_i(a_i^\dagger)$, $b_i(b_i^\dagger)$ are bosonic annihilation (creation) operators of the two species on site i in the Wannier representation, and $n_{ai} \equiv a_i^\dagger a_i$, $n_{bi} \equiv b_i^\dagger b_i$. The first term in Eq. (1) describes the kinetic energy of each species with hopping amplitudes t_a and t_b; the second and the third term represent the on-site inter-species interaction U and the intra-species interactions V_a and V_b for species a and b, respectively; finally, μ_a and μ_b denote the chemical potentials.

Previous studies on two-component ultracold bosons in a square or a cubic optical lattice have revealed a rich phase diagram [10]. Within the Mott insulator, at low temperature quantum magnetism arises, in particular z-antiferromagnetic and xy-ferromagnetic order. For total filling one, the emergence of magnetic order can be easily understood if we note that in the deep Mott regime (strong coupling limit) $t_{a,b} \ll U, V_{a,b}$, the physics of the two-component Bose-Hubbard Hamiltonian (1) is given by an effective spin-1/2 XXZ model [10–12]

$$H_{\text{eff}} = J_z\sum_{\langle ij\rangle} S_i^z S_j^z - J_\perp \sum_{\langle ij\rangle}(S_i^x S_j^x + S_i^y S_j^y) - h\sum_i S_i^z \quad (2)$$

where $\mathbf{S}_i \equiv (a_i^\dagger, b_i^\dagger)(\boldsymbol{\sigma}/2)\begin{pmatrix} a_i \\ b_i \end{pmatrix}$ with $\sigma_x, \sigma_y, \sigma_z$ being the Pauli matrices and

$$J_z = 2\frac{t_b^2 + t_a^2}{U} - \frac{4t_a^2}{V_a} - \frac{4t_b^2}{V_b}, \quad (3)$$

$$J_\perp = \frac{4t_a t_b}{U}, \quad (4)$$

$$h = \frac{2t_a^2}{V_a} - \frac{2t_b^2}{V_b} + (\mu_a - \mu_b). \quad (5)$$

In the following discussion, we assume $h = 0$, i.e. vanishing spin imbalance (in the case of asymmetric hopping $t_a \neq t_b$, the chemical potentials μ_a and μ_b are tuned to achieve this). On bipartite lattices (e.g. square, cubic) the system supports xy-ferromagnetic order for $J_\perp > J_z > 0$, which is characterized by the local correlator $\langle a^\dagger b\rangle$, and z-antiferromagnetic order for $J_z > J_\perp > 0$, characterized by the order parameter $\Delta_{\rm af} = |\langle S_\alpha^z\rangle - \langle S_{\bar\alpha}^z\rangle|$ with α ($\alpha = -\bar\alpha$) being the sublattice index.

We expect new interesting physics to emerge in a system with triangular instead of bipartite optical lattice. For antiferromagnetic exchange coupling J_z, it is impossible to minimize the energy of the spin configuration on each lattice bond, i.e. geometric frustration arises and the system may develop exotic phases at low temperature. We are particularly interested in the extremely asymmetric hopping regime for the full range of couplings from Mott insulator to superfluid. Since higher order density fluctuations of the "lighter" species are expected to become even larger than the low-order density fluctuation of the "heavier" ones, their interplay with Ising-type frustration in z allows the system to form novel phases. Also frustration is expected to grow with increasing values of the hopping amplitudes since the exchange coupling arises from the itinerancy of atoms. In the following, we shall address these two aspects by mapping out the ground state phase diagram for total filling one per site via BDMFT.

Before going into a detailed discussion of the system's properties, let us at this point briefly introduce Bosonic Dynamical Mean Field Theory (BDMFT) [7–9], which is an extension of Dynamical Mean Field Theory (DMFT) [13, 14], originally developed to treat strongly correlated fermionic systems. It is non-perturbative, captures local quantum fluctuations exactly and becomes exact in the infinite-dimensional limit. Note that for antiferromagnetic exchange J_z the ground state of the system may break the translational symmetry of the lattice. We investigate this system using real-space BDMFT (R-BDMFT) [15], which is a generalization of BDMFT to a position-dependent self-energy and captures inhomogeneous quantum phases. Within BDMFT/R-BDMFT, the physics on each lattice site is determined from a local effective action which is obtained by integrating out all the other degrees of freedom in the lattice model, excluding the lattice site considered. The local effective action is then represented by an Anderson impurity model [7–9]. We use Exact Diagonalization (ED) [16, 17] of the effective Anderson Hamiltonian with a finite number of bath orbitals to solve the local action ($n_{\rm bath} = 4$ bath orbitals are chosen in the current work). Details of the R-BDMFT method have been published previously [15].

III. RESULTS

Since we are mainly interested in the effects of geometric frustration, we focus on the parameter regime $V_a = V_b \gg U$, where the leading exchange couplings become Ising antiferromagnetic for highly asymmetric hopping, resulting in Ising-type frustration. In our simulations, the chemical potentials μ_a and μ_b are tuned to equal particle number of both species ($N_a \equiv \sum_i \langle n_{ia}\rangle = N_b \equiv \sum_i \langle n_{ib}\rangle$) and a total filling factor $\rho = \sum_i \langle n_{ia} + n_{ib}\rangle / N_{\rm lat} = 1$ ($N_{\rm lat}$ is the number of lattice sites.). The full range of interactions from strong coupling, deep in the Mott phase, all the way to the superfluid at weak coupling is investigated within BDMFT.

Our main results are summarized in Fig. 1a, which shows the ground state phase diagram for large intra-species interaction strengths ($V_{a,b}/U = 48$). Two different magnetic phases are found in the Mott insulator. When t_a and t_b are of comparable magnitude, the leading exchange coupling is ferromagnetic in the xy-plane, and the system is in the xy-ferromagnetic phase, characterized by a uniform magnetization in the xy-plane. On the other hand, for sufficiently large asymmetry between the two hopping amplitudes, we observe two types of spin-density wave (SDW) phases (see insets (a.1) and (a.2) in Fig. 1a), which break the translation symmetry of the lattice. All of these spin-ordered phases are found to persist up to the superfluid transition. For large hopping the ground state breaks $U(1)$ symmetry and develops superfluid order $\langle a\rangle$,$\langle b\rangle$. Depending on the relative magnitude of t_a and t_b, the system can also exhibit additional charge-density wave order in each species, leading to a supersolid. In the following subsections we discuss detailed properties of the different phases.

A. Spin-density wave (SDW) in the Mott-insulator region

Let us now discuss the origin of the two different SDW phases found in the asymmetric hopping regime.

1. *"3-sublattice" SDW*

In the less asymmetric hopping regime of the SDW phase region (yellow area in the phase diagram Fig. 1a), the SDW features a 3-sublattice structure (see Fig. 2b) ordering at the wave vectors $\pm\mathbf{Q} = (\pm 4\pi/3, 0)$. The emergence of this type of SDW can be understood from a spin-wave theory of the spin-1/2 XXZ model (2), which shows that the uniform xy-ferromagnetic phase develops

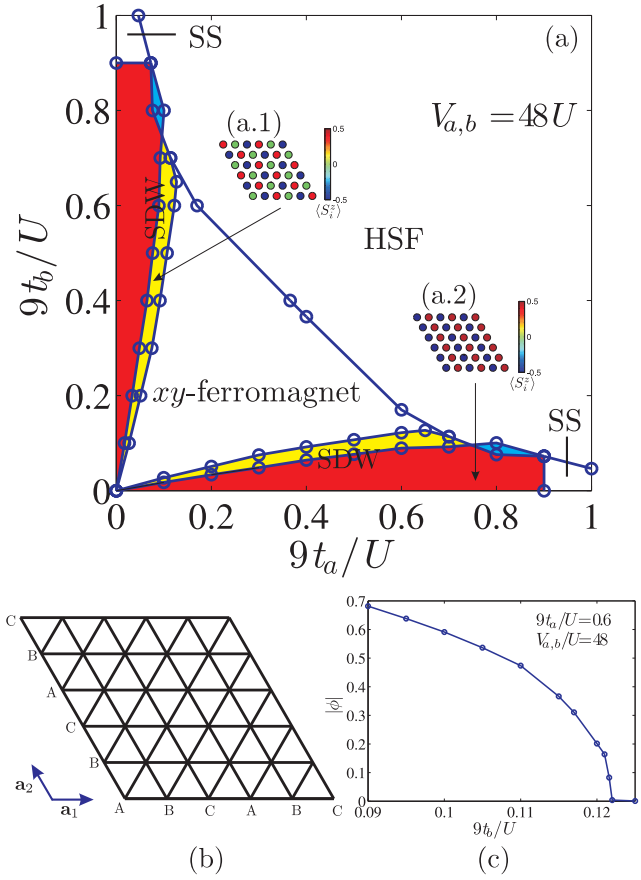

FIG. 1: (Color online) (a) Ground state phase diagram at unit filling $\rho = 1$, with $V_a = V_b = 48U$, obtained from calculations on a 6×6 triangular lattice. We observe four major different phases, which are the homogeneous superfluid (HSF), xy-ferromagnet, spin-density wave (SDW), and supersolid (SS). In the SDW region, the area where the SDW has a 3-sublattice structure is marked in yellow, while the area featuring the stripe SDW is marked red. The insets (a.1) and (a.2) show the corresponding z-magnetization distribution $\langle S_i^z\rangle$. The small blue area indicates a coexistence region of HSF and stripe SDW phases. (b) The triangular lattice considered here with sublattice indices A, B, C marked near the corresponding lattice sites. $\mathbf{a}_1$ and $\mathbf{a}_2$ are the two lattice vectors. (c) t_b dependence of the 3-sublattice SDW order parameter at fixed $9t_a/U = 0.6$.

an instability at $\pm\mathbf{Q} = (\pm 4\pi/3, 0)$ towards 3-sublattice ordering with increasing $J_z/J_\perp$ [18, 19]. Here, we choose the order parameter of the 3-sublattice SDW phase as

$$\phi \equiv \langle S_A^z\rangle + \langle S_B^z\rangle e^{i2\pi/3} + \langle S_C^z\rangle e^{i4\pi/3} \qquad (6)$$

where $\langle S_{A,B,C}^z\rangle$ is the z-magnetization on the sites of the A, B, and C sublattice respectively. ϕ is the Fourier transform of the z-magnetization distribution $\langle S_i^z\rangle$ at the wave vector $\mathbf{Q}$. In Fig. 1b, at fixed t_a, the t_b dependence of $|\phi|$ is shown, indicating a second order phase transition from the 3-sublattice SDW to an xy-ferromagnet.

Let us mention that previous investigations of the spin-1/2 XXZ model in the large $J_z/J_\perp$ region have revealed that the z-magnetization favors a different 3-sublattice patten of $(\langle S_A^z\rangle = \pm 2m, \langle S_B^z\rangle = \mp m, \langle S_C^z\rangle = \mp m)$ in the thermodynamic limit [20, 21], where m is a positive number characterizing the strength of the magnetization. However, although the effective spin-1/2 XXZ model is a reasonable description of the original two-component Bose-Hubbard model (1) in the strong coupling limit, one can not exclude the influence of higher order terms neglected in it. As a matter of fact, even within the spin-1/2 XXZ model itself, although $(\pm 2m, \mp m, \mp m)$ is favored in the thermodynamic limit, a metastable pattern $(\pm m, \mp m, 0)$ is also found in quantum Monte Carlo simulations on finite-sized lattices [20, 21], moreover a variational study shows that the energies corresponding to these two patterns are very close to each other [22]. In our simulations, we find that the system is close to a $(\pm m, \mp m, 0)$ configuration (see Fig. 2b), which could indicate that the effective spin-1/2 XXZ model plus higher order corrections favors this pattern.

2. *Stripe SDW*

In the extremely asymmetric hopping region (area marked in red in the phase diagram Fig. 1a), we observe that another type of SDW phase arises in the system. The z-magnetization distribution is then characterized by a stripe pattern, shown in Fig. 2c. The transition from the stripe SDW phase to the homogeneous superfluid is of first order, which leads to small coexistence regions (blue areas in Fig. 1a).

To understand the appearance of this stripe SDW, we notice that in this regime the hopping amplitude of one species dominates. Without loss of generality, in the following discussion we assume $t_a \gg t_b$, which indicates that the b species can be considered as almost immobile scattering centers. If we assume that the effective spin-1/2 XXZ model (2) description still holds true in this case (in principle the neglected higher order terms may be relevant), the longitudinal exchange coupling J_z is then much larger than the transverse one $J_\perp$, hence the spin-1/2 XXZ model approximately reduces to an antiferromagnetic Ising model. From investigations of the antiferromagnetic Ising model on a triangular lattice [1], we know that the stripe pattern of the magnetization is one of an infinite number of degenerate ground state configurations. However, here we observe no other patterns in our simulation except the stripe configuration. This indicates that for quantitative insight one needs to go beyond the spin-1/2 XXZ model description, which we will do in the following.

We notice that for extremely asymmetric hopping, together with the condition that the intra-species interactions are much larger than the inter-species interactions, i.e. $V_{a,b} \gg U$, the two-component Bose-Hubbard model (1) can be simplified to a bosonic Falicov-Kimball model

with itinerant hard-core bosons

$$H^{\rm BFK} = -\sum_{\langle i,j\rangle}(t_a a_i^\dagger a_j + \text{h.c.}) + U\sum_i n_{ai}n_{bi} - \sum_{i;\alpha=a,b}\mu_\alpha n_{\alpha i}\,. \tag{7}$$

At zero temperature, integrating out the itinerant bosonic degree of freedom under the assumption $t_a \ll U$, we end up with an effective classical spin Hamiltonian representing the density-density interactions of the immobile b species, which is accurate to the order $O(t_a^5/U^4)$ [23] and reads

$$\begin{aligned} H_{\rm eff}^{\rm BFK}(s;\mu_\alpha) \;=\; & -\frac{1}{2}(\mu_b-\mu_a)\sum_i s_i - \frac{1}{2}(\mu_a+\mu_b+U+\frac{3}{2}\frac{t_a^3}{U^2})N_{\rm lat} + \sum_{\langle i,j\rangle}\left[\frac{t_a^2}{4U}+\frac{t_a^3}{4U^2}-\frac{t_a^4}{8U^3}\right]s_i s_j \\ & + \sum_{\langle\langle i,j\rangle\rangle}\frac{5t_a^4}{16U^3}s_i s_j + \sum_{\langle\langle\langle i,j\rangle\rangle\rangle}\frac{t_a^4}{8U^3}s_i s_j - \sum_P \frac{t_a^4}{16U^3}(5+s_P)\,, \end{aligned} \tag{8}$$

where $N_{\rm lat}$ is the number of lattice sites, $\langle\langle i,j\rangle\rangle$ and $\langle\langle\langle i,j\rangle\rangle\rangle$ denote next-nearest neighbor and next-next-nearest neighbor sites respectively (see Fig. 2d). The Ising pseudo spin s_i is defined as $s_i \equiv (-1)^{n_i^b+1}$. P denotes the plaquettes made up of two triangles sharing an edge and $s_P \equiv s_{P1}s_{P2}s_{P3}s_{P4}$ is the product of the spins on all sites in the plaquette. Detailed studies of the model (8) in Ref. [23] show that at the filling $N_a = N_b = N/2$, the ground state of the above classical spin Hamiltonian $H_{\rm eff}^{\rm BFK}(s;\mu_\alpha)$ is non-degenerate and has a stripe pattern configuration of the Ising pseudo spins similar to that observed in our numerical BDMFT simulations. From (8) we observe that in the leading order $O(t_a^2/U)$ the classical spin model shows an Ising-type frustration on the triangular lattice, however the frustration is removed by next-nearest neighbor and next-next-nearest neighbor effective spin interactions which originate from higher-order density fluctuations of the mobile particles (the a species atoms in this case).

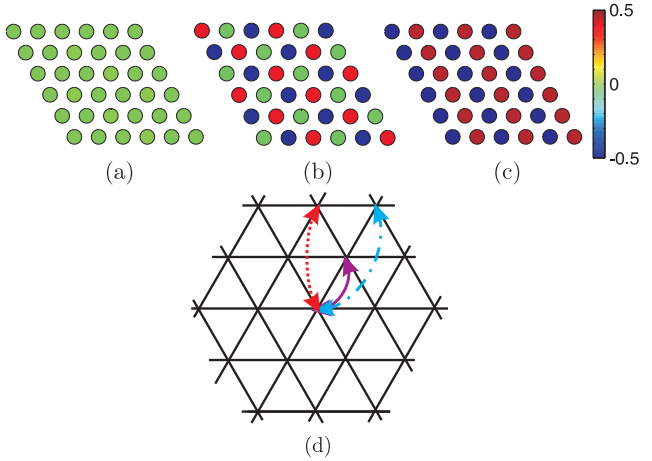

FIG. 2: (Color online) (a–c) z-magnetization distribution $\langle S_i^z\rangle$ for different Mott-insulating phases with quantum magnetic order. (a) xy-ferromagnet for $9t_a/U = 0.6$ and $9t_b/U = 0.14$. (b) 3-sublattice SDW for $9t_a/U = 0.7$ and $9t_b/U = 0.1$. (c) Stripe SDW for $9t_a/U = 0.7$ and $9t_b/U = 0.05$. In all the three cases, we set $V_{a,b}/U = 48$. (d) Schematic figure where nearest neighbor, next-nearest neighbor, and next-next-nearest neighbor sites in a triangular lattice are indicated by the purple solid line, red dashed line, and blue dash-dotted line respectively.

3. *Weak charge-density wave (CDW) on top of SDW phase*

In the the SDW region we also observe a weak charge-density wave (CDW) of the total density $\rho_i = \langle\sum_{\alpha=a,b} n_{\alpha i}\rangle$ forming on top of the SDW (see Fig. 3b). Specifically, we found that for $t_a > t_b$, those lattice sites with a negative z-magnetization have a larger total density ρ_i, while for $t_a < t_b$, those sites with a positive z-magnetization have the larger density.

The origin of this weak CDW can be easily understood by investigating a simplified two-site two-component Bose-Hubbard model

$$\begin{aligned} H_{\rm TT} \;=\; & -(t_a a_L^\dagger a_R + t_b b_L^\dagger b_R + \text{h.c.}) + U\sum_{i=L,R} n_{ai}n_{bi} \\ & + \frac{1}{2}\sum_{i=L,R;\alpha=a,b} V_\alpha n_{i\alpha}(n_{i\alpha}-1)\,. \end{aligned} \tag{9}$$

Since the onsite interaction is much larger than the kinetic energy, we treat the hopping terms as perturbations. Since we are investigating the CDW on top of the SDW, we assume a simple symmetry-broken state $\left|\Psi_G^{(0)}\right\rangle = a_L^\dagger b_R^\dagger|0\rangle$ as the unperturbed ground state, which implies that the L and R sites have equal total density ($\rho_L = \rho_R = 1$) but opposite z-magnetization ($\langle S_L^z\rangle = -\langle S_R^z\rangle = 1/2$). If we take into account the hopping terms to first order, the ground state has the form

$$\left|\Psi_G^{(1)}\right\rangle = \frac{U a_L^\dagger b_R^\dagger|0\rangle + t_b a_L^\dagger b_L^\dagger|0\rangle + t_a a_R^\dagger b_R^\dagger|0\rangle}{\sqrt{U^2+t_a^2+t_b^2}}, \tag{10}$$

and the total density on the site L and R is

$$\rho_L \approx 1-\delta, \quad (11)$$
$$\rho_R \approx 1+\delta, \quad (12)$$

where $\delta = (t_a^2 - t_b^2)/(U^2 + t_a^2 + t_b^2)$, indicating that the weak CDW order on top of the SDW originates from the asymmetry of the hopping amplitudes, i.e. the "lighter" species can more easily delocalize to neighboring sites. Fig. 3 shows the amplitudes of the stripe SDW and the CDW orders as a function of t_a at fixed t_b. Those amplitudes are defined by $\delta\rho \equiv \rho_+ - \rho_-$ and $S^z_{\rm stripe} \equiv S^z_+ - S^z_-$ for CDW and SDW order respectively, where $\rho_+(\rho_-)$ is the total particle density per site on the stripe with higher (lower) density and $S^z_+(S^z_-)$ is the z-magnetization per site on the stripe with positive (negative) value.

More generally we can analyze the emergence of the CDW within a Ginzburg-Landau framework. We assume spin density wave order at wavevectors $\mathbf{Q}$ and $-\mathbf{Q}$, and study its interaction with a putative CDW order parameter. The lattice translation and Ising spin symmetries of the problem determine the allowed coupling terms that affect the CDW order, given in the following expansion of the free energy

$$\begin{aligned} F \;=\; & \alpha_s|S^z_{\mathbf{Q}}|^2 + \alpha_{\rho 1}|\rho_{\mathbf{Q}}|^2 + \alpha_{\rho 2}|\rho_{2\mathbf{Q}}|^2 \\ & +\beta_1(S^z_{\mathbf{Q}}S^z_{\mathbf{Q}}\rho_{-2\mathbf{Q}} + \text{h.c.}) \\ & +\beta_2|S^z_{\mathbf{Q}}|^2|\rho_{\mathbf{Q}}|^2 + \beta_3\left[(S^z_{-\mathbf{Q}})^2(\rho_{\mathbf{Q}})^2 + \text{h.c.}\right] \\ & +\gamma_s|S^z_{\mathbf{Q}}|^4 + \gamma_{\rho 1}|\rho_{\mathbf{Q}}|^4 + \gamma_{\rho 2}|\rho_{2\mathbf{Q}}|^4, \end{aligned} \quad (13)$$

where the α's, β's, and γ's are GL coefficients. The crucial point is that symmetry allows a linear coupling of a charge density wave at $\pm 2\mathbf{Q}$ to the square of the SDW order parameter (coupling β_1 above). Therefore a SDW order at $\pm\mathbf{Q}$ will necessarily produce CDW at $\mp 2\mathbf{Q}$. The opposite is not true, that is CDW order will not produce SDW in general. This is because a quadratic-linear coupling to the SDW is prohibited by the Ising spin symmetry.

Let us first describe the implications of this fact in the case of the 3-sublattice SDW with wavevector $\mathbf{Q} = (\pm 4\pi/3, 0)$. In this case the CDW induced by the cubic coupling is of wavevector $-2\mathbf{Q} = -\text{sgn}(Q_x)(4\pi, 0) + \mathbf{Q}$, which in the lattice is equivalent to $\mathbf{Q}$. This explains, from a very general argument, why a CDW at $\mathbf{Q}$ must be produced in this case.

Let us move on to consider the case of the stripe SDW having a wavevector $\mathbf{Q} = \pm\mathbf{K}/2$ with $\mathbf{K}$ being a reciprocal lattice vector. The coupling to $\rho_{2\mathbf{Q}}$ is then equivalent on the lattice to a coupling to the average density $\rho_{\mathbf{Q}=0}$ that can be absorbed into the chemical potential term. As a consequence, the only non-trivial CDW's are the ones at $\pm\mathbf{Q}$ and induced by the SDW order at $\pm\mathbf{Q}$ through the next order terms quadratic in the CDW.

To briefly summarize, both 3-sublattice SDW and stripe SDW induce CDW at the same wave vector, which is consistent with our simulations (see Fig. 3b, which shows a stripe SDW with a large SDW order induces a CDW at the same wave vector). However, in the case of a stripe SDW the CDW is induced by coupling to $|\rho_{\mathbf{Q}}|^2$ rather than by linear coupling. It therefore requires a critical strength of the stripe SDW to change the sign of the coefficient of $|\rho_{\mathbf{Q}}|^2$ and induce CDW order.

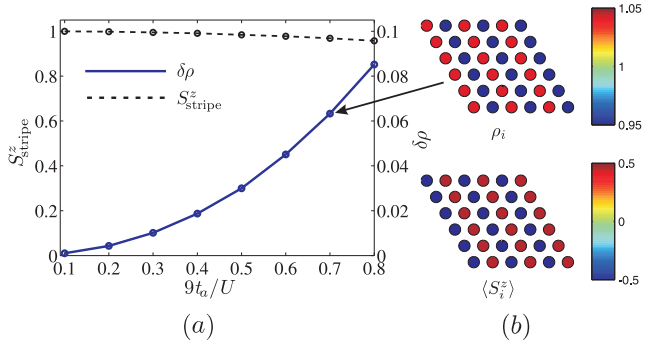

FIG. 3: (Color online) (a) In the stripe SDW phase region, we show the CDW order (blue solid line) and SDW order (black dashed line) as a function of t_a when $9t_b/U = 0.01$ is kept fixed. (b) The total density (ρ_i) (upper panel) and the z-magnetization ($\langle S^z_i\rangle$) distribution (lower panel) for $V_{a,b}/U = 48$, $9t_a/U = 0.7$, and $9t_b/U = 0.01$.

B. Superfluid and supersolid in the large-hopping region

At sufficiently large hopping amplitudes, the ground state of the system breaks $U(1)$ symmetry and develops superfluid long-range order characterized by nonzero values of $\langle a\rangle$ or $\langle b\rangle$. In the region where the hopping amplitudes t_a and t_b are comparable to each other, we observe a second order phase transition from xy-ferromagnetism to the homogeneous superfluid (HSF). On the other hand, for highly asymmetric t_a and t_b, increasing the hopping amplitudes can first drive the system from the SDW into a supersolid, which is characterized by coexisting superfluid and CDW order. In the supersolid phase, the lighter species develops superfluid order, i.e. $\langle\alpha\rangle \neq 0$, while the heavier species remains insulating, i.e. $\langle\bar{\alpha}\rangle = 0$, where $\alpha(\bar{\alpha})$ denote the annihilation operator of the lighter/heavier species and both species have CDW order in their density distribution respectively. When the hopping amplitudes are further increased, a transition from the supersolid to a homogeneous superfluid is observed.

IV. CONCLUSION

We have investigated zero temperature quantum phases of Bose-Bose mixtures in a triangular lattice using real-space Bosonic Dynamical Mean Field Theory. A rich phase diagram including xy-ferromagnet, spin-density wave, superfluid, and supersolid phases is found.

In the strong coupling regime, although an effective spin-1/2 XXZ model gives qualitative insight, interesting phases beyond this effective description are found: A stripe spin-density wave is identified for highly asymmetric hopping, which originates from the interplay between classical geometric frustration and higher order density fluctuations of the lighter species. Moreover, on top of the spin-density wave, due to asymmetric hopping amplitudes, the system shows a weak charge-density wave in the total particle density distribution.

Acknowledgments

L. He acknowledges useful discussions with S. D. Huber, A. Sotnikov, D. Cocks and I. Titvinidze and the hospitality of the Department of Condensed Matter Physics, Weizmann Institute of Science, where parts of this work were done. This work was supported by the Deutsche Forschungsgemeinschaft via the DIP project HO 2407/5-1, Sonderforschungsbereich SFB/TR 49, Forschergruppe FOR 801, ISF grant 1594/11 (E. A.) and by the China Scholarship Fund (Y. L.). W. H. acknowledges the hospitality of KITP during the final stages of this work, supported by the National Science Foundation under Grant No. NSF PHY05-51164.

[1] G. H. Wannier, Phys. Rev. **79**, 357 (1950).
[2] R. Moessner and A. P. Ramirez, Phys. Today **59(2)**, 24 (2006).
[3] S. Sachdev, Nat. Phys. **4**, 173 (2008).
[4] C. Becker, P. Soltan-Panahi, J. Kronjäger, S. Dörscher, K. Bongs, K. Sengstock, New J. Phys. **12**, 065025 (2010).
[5] J. Struck, C. Ölschläger, R. L. Targat, P. Soltan-Panahi, A. Eckardt, M. Lewenstein, P. Windpassinger, K. Sengstock, Science **333**, 996 (2011).
[6] G. B. Jo, J. Guzman, C. K. Thomas, P. Hosur, A. Vishwanath, D. M. Stamper-Kurn, Phys. Rev. Lett. **108**, 045305 (2012).
[7] K. Byczuk and D. Vollhardt, Phys. Rev. B **77**, 235106 (2008).
[8] A. Hubener, M. Snoek, and W. Hofstetter, Phys. Rev. B **80**, 245109 (2009).
[9] W. J. Hu and N. H. Tong, Phys. Rev. B **80**, 245110 (2009).
[10] E. Altman, W. Hofstetter, E. Demler and M. Lukin, New J. Phys. **5**, 113 (2003).
[11] A. B. Kuklov and B. V. Svistunov, Phys. Rev. Lett. **90**, 100401 (2003).
[12] L. M. Duan, E. Demler, and M. D. Lukin, Phys. Rev. Lett. **91**, 090402 (2003).
[13] W. Metzner and D. Vollhardt, Phys. Rev. Lett. **62**, 324 (1989).
[14] A. Georges, G. Kotliar, W. Krauth, and M. J. Rozenberg, Rev. Mod. Phys. **68**, 13 (1996).
[15] Y. Q. Li, M. R. Bakhtiari, L. He, and W. Hofstetter, Phys. Rev. B **84**, 144411 (2011).
[16] M. Caffarel and W. Krauth, Phys. Rev. Lett. **72**, 1545 (1994).
[17] Q.-M. Si, M. J. Rozenberg, G. Kotliar, and A. E. Ruckenstein, Phys. Rev. Lett. **72**, 2761 (1994).
[18] G. Murthy, D. Arovas, and A. Auerbach, Phys. Rev. B **55**, 3104 (1997).
[19] R. G. Melko, A. Paramekanti, A. A. Burkov, A. Vishwanath, D. N. Sheng, and L. Balents, Phys. Rev. Lett. **95**, 127207 (2005).
[20] S. Wessel and M. Troyer, Phys. Rev. Lett. **95**, 127205 (2005).
[21] M. Boninsegni and N. Prokof'ev, Phys. Rev. Lett. **95**, 237204 (2005).
[22] A. Sen, P. Dutt, K. Damle, and R. Moessner, Phys. Rev. Lett. **100**, 147204 (2008).
[23] C. Gruber, N. Macris, and A. Messager, J. Stat. Phys. **86** 57 (1997).